

Cosmological constraints on deviations from Lorentz invariance in gravity and dark matter

B. Audren^a, D. Blas^b, M. M. Ivanov^{c,d,f}, J. Lesgourgues^{a,b,e}, S. Sibiryakov^{a,b,d}

^a *FSB/ITP/LPPC, École Polytechnique Fédérale de Lausanne,
CH-1015, Lausanne, Switzerland*

^b *Theory Group, Physics Department, CERN, CH-1211 Geneva 23, Switzerland*

^c *Faculty of Physics, Moscow State University, Vorobjevy Gory, 119991 Moscow, Russia*

^d *Institute for Nuclear Research of the Russian Academy of Sciences,
60th October Anniversary Prospect, 7a, 117312 Moscow, Russia*

^e *LAPTH, U. de Savoie, CNRS, BP 110, 74941 Annecy-Le-Vieux, France and*

^f *Sternberg Astronomical Institute, Universitetsky prospect, 13, 119992 Moscow, Russia*

We consider a scenario where local Lorentz invariance is violated by the existence of a preferred time direction at every space-time point. This scenario can arise in the context of quantum gravity and its description at low energies contains a unit time-like vector field which parameterizes the preferred direction. The particle physics tests of Lorentz invariance preclude a direct coupling of this vector to the fields of the Standard Model, but do not bear implications for dark matter. We discuss how the presence of this vector and its possible coupling to dark matter affect the evolution of the Universe. At the level of homogeneous cosmology the only effect of Lorentz invariance violation is a rescaling of the expansion rate. The physics is richer at the level of perturbations. We identify three effects crucial for observations: the rescaling of the matter contribution to the Poisson equation, the appearance of an extra contribution to the anisotropic stress and the scale-dependent enhancement of dark matter clustering. These effects result in distinctive features in the power spectra of the CMB and density fluctuations. Making use of the data from Planck and WiggleZ we obtain the most stringent cosmological constraints to date on departures from Lorentz symmetry. Our analysis provides the first direct bounds on deviations from Lorentz invariance in the dark matter sector.

I. INTRODUCTION

Understanding the properties of the different components of the Universe is one of the major aims of cosmology and particle physics. All current data are compatible with the Λ CDM scenario, where the fields of the Standard Model of particle physics (SM) are supplemented by a dark matter component and a cosmological constant. This scenario assumes that Lorentz invariance (LI) is a fundamental property of Nature, and thus holds for all sectors of the theory. As for any postulate, it is important to verify this assumption experimentally. Indeed, many tests have been performed within SM establishing the validity of LI in this sector with exquisite accuracy [1, 2]. On the other hand, the tests of LI in gravity are mostly limited to the framework of the post-Newtonian expansion and are based on the observations in a rather narrow range of distances relevant for the planetary and stellar dynamics [3]. The probes going beyond the post-Newtonian description, such as the study of energy loss rate by binary pulsars, are able to give only mild bounds on deviations from LI in gravity [4]. Moreover, we do not have any direct information about the validity of LI in the dark sectors of the Universe: dark matter and dark energy. Given the key role played by LI in describing Nature it is essential to test it at all accessible scales for as many observables as possible.

Further motivation to consider Lorentz invariance violation (LV) comes from the quest for a theory of quantum gravity. A concrete scenario in this direction is Hořava

gravity [5, 6], where the ultraviolet behavior of the gravitons is modified by operators breaking LI; this leads to a power counting renormalizable theory. In a broader perspective, one could envisage that the theory of quantum gravity would generate LV at low-energies, which one could parameterize using effective theories, such as the Einstein-aether model [7] or the SM extension of particle physics [8]. These theories generically include extra massless excitations in the gravity sector which yield a very rich phenomenology beyond general relativity (GR) at all scales, in particular, in cosmology. Given the remarkable progress in the amount and quality of the cosmological data during recent years, it is reasonable to ask if they can provide information about the validity of LI in gravity and the dark sectors. This topic was first addressed in [9] where LV in gravity parameterized by the Einstein-aether model was constrained using the data on cosmic microwave background (CMB) and large scale structure (LSS). More recently [10] considered a scenario with LV in gravity and dark energy sectors, which presents an alternative to Λ CDM where cosmic acceleration is sourced by a term insensitive to large ultraviolet corrections [11].

The purpose of this paper is to use the recent results on the CMB [12] and linear matter power spectrum (LPS) [13] to constrain the deviations with respect to Λ CDM associated with LV in gravity and *dark matter*. We will focus on the effects from the existence of a preferred time-direction. Our study is based on the phenomenological description of LV in dark matter developed in [14].

The paper is organized as follows. In Sec. II we sum-

marize the formalism for the effective description of LV in gravity and dark matter. We discuss the cosmological background evolution and present the equations for the perturbations in Sec. III. In Sec. IV we describe the effects of LV on the CMB and LPS. Sec. V contains the main results of the paper: the observational constraints on the LV parameters. We conclude in Sec. VI.

II. LORENTZ BREAKING THEORIES OF GRAVITY AND DARK MATTER

We assume that the Universe is permeated by a time-like vector field u_μ — “aether” — defining a preferred time direction at every point of space-time. This vector is taken to have unit norm¹,

$$u_\mu u^\mu = -1. \quad (1)$$

The presence of this field breaks LI locally down to spatial rotations. The covariant action for u_μ and the metric $g_{\mu\nu}$ with the minimum number of derivatives reads,

$$S_{[\text{EHu}]} = \frac{1}{16\pi G_0} \int d^4x \sqrt{-g} [R - K^{\mu\nu}{}_{\sigma\rho} \nabla_\mu u^\sigma \nabla_\nu u^\rho + l(u_\mu u^\mu + 1)], \quad (2)$$

where R is the Ricci scalar for the metric $g_{\mu\nu}$,

$$K^{\mu\nu}{}_{\sigma\rho} \equiv c_1 g^{\mu\nu} g_{\sigma\rho} + c_2 \delta_\sigma^\mu \delta_\rho^\nu + c_3 \delta_\rho^\mu \delta_\sigma^\nu - c_4 u^\mu u^\nu g_{\sigma\rho}, \quad (3)$$

and l is a Lagrange multiplier that enforces the unit-norm constraint. This is the action of the Einstein-aether model [7, 15]. The parameter G_0 in (2) is related to Newton’s constant as [6, 15]

$$G_N \equiv G_0 (1 - (c_4 + c_1)/2)^{-1}. \quad (4)$$

The dimensionless constants c_a , $a = 1, 2, 3, 4$, characterize the strength of the interaction of the aether u_μ with gravity.

One can require additionally that the field u_μ is orthogonal to a family of three-dimensional hypersurfaces defined as the leaves of constant scalar field φ ,

$$u_\mu \equiv \frac{\partial_\mu \varphi}{\sqrt{-\partial^\nu \varphi \partial_\nu \varphi}}. \quad (5)$$

Then the action (2) corresponds to the *khronometric* model which represents the low-energy limit of Hořava gravity [6, 16]. In this case the term with the Lagrange multiplier is redundant and the four terms in (3) are linearly dependent. Thus $K^{\mu\nu}{}_{\sigma\rho}$ can be reduced to its last three terms with coefficients

$$\lambda \equiv c_2, \quad \beta \equiv c_3 + c_1, \quad \alpha \equiv c_4 + c_1. \quad (6)$$

¹ We use the $(-+++)$ signature for the metric and work in units $\hbar = c = 1$.

The detailed relation between the Einstein-aether and khronometric models has been worked out in [17].

The previous action should be supplemented by an action for the matter sector. This consists of the SM part and a dark matter (DM) component. Generically, both can be directly coupled to the vector u_μ . For the SM part, this coupling is strongly constrained from tests of LI in particle physics experiments [1, 2] and checks of the weak equivalence principle [3], which implies that it is negligible in cosmology. In what follows we assume that there is no direct coupling between SM and the aether. This decoupling can be ensured, e.g., by imposing (softly broken) supersymmetry [18, 19] or by a dynamical emergence of LI at low energies in the SM sector [20]. In contrast, these mechanisms do not work for particles that are singlets under the gauge group (in the case of supersymmetry) or for weakly coupled particles (in the case of dynamical emergence). As DM must be weakly interacting with SM and is conventionally believed to be a gauge singlet, its coupling to the aether can be sizeable.

Since the relation between dark DM and SM particles is not established, the only direct tests of LV in DM can come from cosmological analysis. For DM, the possibility of a direct coupling to u_μ was first considered in [14]. It was shown that within the fluid description of DM this coupling leads to the following effective action,

$$S_{[\text{DMu}]} = -m \int d^4x \sqrt{-g} n F(u_\mu v^\mu), \quad (7)$$

where m is the mass of the DM particles², n is their number density and v^μ is their four-velocity. The function $F(u_\mu v^\mu)$ parameterizes the interaction between the DM fluid and the aether; without loss of generality, it can be normalized to $F(1) = 1$. We will see below that the effect on cosmology is encapsulated by a single parameter,

$$Y \equiv F'(1). \quad (8)$$

In particle physics LV is usually associated with the modification of the particles’ dispersion relations — the dependence of their energy on the spatial momentum. The effective field theory framework predicts that at relatively low energies the leading modification occurs in the quadratic term [21], giving

$$E^2 = m^2 + (1 + \xi) \mathbf{p}^2, \quad (9)$$

where for a relativistic theory $\xi = 0$. Requiring that the DM particles have the dispersion relation (9) in the rest frame of the aether (i.e. where it has the form $u_\mu = (1, 0, 0, 0)$) corresponds to choosing a function F in (7)

² As explained in [14], this framework can be generalized almost without changes to the case of any DM admitting a fluid description, such as, for example, axionic DM. We stick in this paper to the simple physical picture of weakly interacting massive particles for concreteness.

with $Y = \xi/(1 + \xi)$ [14]. Thus, by putting bounds on the parameter Y we will be able to constrain the deviations of the DM dispersion relation from the relativistic form.

In deriving the equations of motion following from (7) the variation of the fields must be subject to the constraints³ $v^\mu v_\mu = -1$, $\nabla_\mu(n v^\mu) = 0$, the latter expressing the particle number conservation. The resulting equations for the aether-DM system can be found in [14].

Finally, we add to the total energy budget of the Universe the cosmological constant Λ as the source of the cosmic acceleration. We will refer to the resulting cosmological model as Λ LVDM.

Various combinations of the parameters introduced above are constrained by experiment. Despite the fact that the aether does not couple directly to SM, it affects the gravitational interactions among celestial bodies. The Solar System tests provide the bounds $|\alpha_1| \lesssim 10^{-4}$ and $|\alpha_2| \lesssim 10^{-7}$, where α_1, α_2 are certain combinations of the parameters c_a entering in the post-Newtonian dynamics [15, 16, 24]. Since these bounds are much stronger than those expected from cosmology, we will impose vanishing of α_1, α_2 as priors in our parameter extraction procedure. In terms of the original coefficients this amounts to imposing the following relations⁴:

- for Einstein-aether model:

$$c_1 c_4 + c_3^2 = 0, \quad (10a)$$

$$2c_1 + 3c_2 + c_3 + c_4 = 0; \quad (10b)$$

- for khronometric model:

$$\alpha - 2\beta = 0. \quad (11)$$

Remarkably, in the khronometric case a single relation (11) suffices to ensure vanishing of all post-Newtonian (PN) parameters.

A stringent bound $|\hat{\alpha}_2| \lesssim 10^{-9}$ has been derived from the dynamics of solitary pulsars [25], where $\hat{\alpha}_2$ is the generalization of α_2 for strong gravitational fields. However, this translates in rather mild constraints on the parameters of the model once the vanishing of the PN parameters, eqs. (10b) or (11), is imposed [4]. Stronger constraints follow from the radiation damping in binary systems [4], which is an efficient way to test LV beyond the combinations α_1 and α_2 . Except for some degeneracies, these bounds are of order $|c_a| \lesssim 10^{-2}$. Besides, there are theoretical constraints that further restrict the allowed parameter space, see e.g. [4] for a succinct re-

view. In particular, stability imposes the following positivity conditions on the combinations (6),

$$0 < \alpha < 2, \quad 0 < \beta + \lambda. \quad (12)$$

A future direct detection of DM, implying its appreciable coupling to the SM fields, can lead to strong constraints on the DM – aether interaction. In this case, following the arguments of [26, 27] one would be able to estimate the direct coupling of SM to u_μ induced by radiative corrections due to DM loops and apply the stringent constraints on LV in SM. However, these bounds will be model-dependent and, in the absence of a direct DM detection so far, we do not take them into account in the present work.

III. COSMOLOGICAL BACKGROUND AND PERTURBATIONS

It was shown in [14] that the only effect of the previous modifications for homogeneous and isotropic backgrounds is a rescaling of the gravitational constant in the Friedmann equation⁵

$$G_{cos} \equiv G_0 \left[1 + \frac{c_1 + 3c_2 + c_3}{2} \right]^{-1}. \quad (13)$$

This does not coincide with the Newton's constant governing local gravity (4). Since G_{cos} affects the relic abundance of different elements in the Universe, it can be constrained with the Big Bang Nucleosynthesis (BBN) data [28]. Note, however, that in the Einstein-aether case the condition for vanishing of the post-Newtonian parameters (10b) implies that G_{cos} coincides with G_N to the linear order in the aether parameters c_a and the BBN constraints are weakened.

For the perturbations, we will focus on the scalar sector of the theory⁶. The dynamic of this sector is identical in the Einstein-aether and khronometric cases and depends only on the combinations (6). We work in the synchronous gauge [31] where the metric takes the form,

$$ds^2 = a^2(\tau) \left[-d\tau^2 + \left(\delta_{ij} + \frac{\partial_i \partial_j}{\Delta} h + 6 \left(\frac{\partial_i \partial_j}{\Delta} - \frac{\delta_{ij}}{3} \right) \eta \right) dx^i dx^j \right], \quad (14)$$

where $\Delta \equiv \partial_i \partial_i$ is the spatial Laplacian. Given eq. (1), the scalar perturbations of the field u_μ can be parametrised as

$$u_0 = a(\tau), \quad u_i = a(\tau) \partial_i \chi. \quad (15)$$

³ Alternatively, within the so-called pull-back formalism, one introduces a triple of scalar fields parameterizing the fluid elements and varies with respect to these fields without any restrictions [14, 22, 23].

⁴ The difference between the Einstein-aether and khronometric models is due to the helicity-1 perturbations in the Einstein-aether case, which contribute into α_1, α_2 .

⁵ In particular, the introduction of the aether and its interaction with DM cannot, by itself, provide the present accelerated expansion of the universe. More ingredients can be added to this setup to realize dark energy in a technically natural way [10].

⁶ Vectors may be important in the Einstein-aether case [29, 30] if they are efficiently produced in the primordial Universe and do not decay with time. This happens in a restricted portion of the parameter space.

In Fourier space, the DM equations read

$$\dot{\delta}_{[dm]} + \theta_{[dm]} + \frac{\dot{h}}{2} = 0, \quad (16a)$$

$$\dot{\theta}_{[dm]} + \mathcal{H}\theta_{[dm]} + \frac{Yk^2}{1-Y}(\dot{\chi} + \mathcal{H}\chi) = 0, \quad (16b)$$

where dot stands for the derivatives with respect to the conformal time τ ; $\mathcal{H} \equiv \dot{a}/a$; the DM density contrast and velocity divergence are defined in the usual way,

$$\delta_{[dm]} \equiv \frac{\delta\rho_{[dm]}}{\rho_{[dm]}}, \quad \theta_{[dm]} \equiv \frac{ik_j v_{[dm]}^j}{a(\tau)}, \quad (17)$$

and Y has been defined in (8). Unlike the standard case we cannot put the DM velocity to zero by a residual gauge choice. The reason is that, due to the interaction with the aether, DM does not follow geodesics. Instead, from (16b) we see that we can impose

$$\theta_{[dm]} = -\frac{Yk^2}{1-Y}\chi. \quad (18)$$

In this gauge the equations for u_μ reduce to

$$\ddot{\chi} = -\frac{c_\chi^2}{2}\dot{h} - 2\frac{\beta}{\alpha}\dot{\eta} - 2\mathcal{H}\dot{\chi} - \left[(1+B)\mathcal{H}^2 + (1-B)\dot{\mathcal{H}} + c_\chi^2 k^2 + \frac{c_\chi^2 k_{Y,0}^2}{a} \right] \chi, \quad (19)$$

with $B \equiv \frac{\beta+3\lambda}{\alpha}$,

$$c_\chi^2 \equiv \frac{\beta+\lambda}{\alpha}, \quad k_{Y,0}^2 \equiv \frac{3Y\Omega_{dm}H_0^2}{(\beta+\lambda)(1-Y)} \frac{G_0}{G_{\text{cos}}}, \quad (20)$$

where Ω_{dm} is the dark matter fraction and H_0 is the Hubble parameter today. The constant c_χ^2 has the physical meaning of the squared velocity of the longitudinal aether waves, its positivity is guaranteed by the conditions (12). From theoretical viewpoint, c_χ can be both smaller or larger than unity: superluminal propagation is compatible with causality in the presence of LV. Importantly, the absence of energy losses by ultra-high energy cosmic rays via vacuum Cherenkov emission of the χ -field requires that c_χ must be equal or bigger than 1 [32].⁷ We will impose this requirement as a prior in our parameter extraction procedure.

The last term in the square brackets in (19) effectively introduces a (time-dependent) mass for the aether perturbations. We impose a theoretical prior that the square of this mass must be positive, $k_{Y,0}^2 > 0$ — otherwise one expects rapid instabilities in the aether–DM sector [14]

in contradiction with observations. Thus in what follows we restrict to

$$0 \leq Y < 1. \quad (21)$$

On the other hand, the positive effective mass leads to the suppression of the aether perturbations for $k < k_{Y,0}/\sqrt{a(\tau)}$ implying that LV effects are screened at distances longer than $2\pi k_{Y,0}^{-1}$ [14].⁸

Finally, the only two independent equations following from the linearized Einstein equations are,

$$k^2\eta - \frac{1}{2}\frac{G_0}{G_{\text{cos}}}\mathcal{H}\dot{h} = -4\pi a^2 G_0 \sum_i \rho_i \delta_i - \alpha k^2 (\mathcal{H}(1-B)\chi + \dot{\chi}), \quad (22)$$

$$\ddot{h} = -2\mathcal{H}\dot{h} + \frac{G_{\text{cos}}}{G_0} 2k^2\eta - 24\pi a^2 \sum_i \delta p_i - \alpha B \frac{G_{\text{cos}}}{G_0} k^2 (\dot{\chi} + 2\mathcal{H}\chi), \quad (23)$$

where the sums on the r.h.s. run over the matter species filling the Universe: DM, baryons and radiation (including neutrinos, which we assume to be massless). The system is completed by the standard equations for the baryon and radiation components [31].

To solve the previous equations for a given Fourier mode k we set the initial conditions in the radiation era, at a moment τ_0 when the wavelength associated to k is well outside the Hubble scale, i.e. when $k \ll \mathcal{H}$. These modes will be initiated in the adiabatic growing mode of the model [14], which under broad assumptions gives the dominant contribution to the perturbations⁹. Further details on the numerical procedure in a similar theory can be found in [10].

IV. EFFECTS ON OBSERVATIONS

Some of the cosmological effects of LV were discussed in the past [9, 10, 14, 28, 29, 33]. Here we summarize

⁸ Note that the definition of $k_{Y,0}$ used in this paper differs from that in [14] by a factor of c_χ^{-2} .

⁹ Isocurvature modes were considered in [11, 14, 29]. In the kronometric case they always decay outside the horizon once the PPN condition (11) is imposed. In the Einstein-aether model they also decay if $Y \neq 0$ and the LV parameters satisfy (10b). Finally, if $Y = 0$ the isocurvature modes stay constant at super-horizon distances in the Einstein-aether case after imposing (10b). Even a small deviation from (10b) means that the modes either grow or decay [11]. Thus, if primordially generated, isocurvature modes can survive only in the Einstein-aether theory with LI DM [29]. We leave the study of their phenomenology for future. It is worth mentioning that the presence of the aether does not necessarily lead to the production of isocurvature modes during inflation. There are examples of inflationary models (see [41]) containing the aether and generating primordial perturbations in pure adiabatic modes.

⁷ More precisely, the bound reads $c_\chi^2 > 1 - 10^{-22}$ as long as the process would occur with sizable probability over the cosmological distances. This is the case as long as $\frac{(\beta-\alpha)^2}{\alpha} > 10^{-30}$.

and extend them emphasizing the effects related to LV in dark matter.

The deviations of Λ LVDM from the standard cosmology can be divided into three categories:

- (i) effects related to the difference between G_N and G_{cos} ; they are proportional to

$$\frac{G_N}{G_{cos}} - 1 = \frac{\alpha + \beta + 3\lambda}{2} + \mathcal{O}(\alpha^2), \quad (24)$$

where by $\mathcal{O}(\alpha^2)$ we mean any subleading contributions in the parameters α, β, λ

- (ii) effects due to the presence of shear; they are proportional to β [14]

- (iii) effects due to LV in DM appearing for non-zero value of the parameter Y .

The first two classes of effects are common to a very broad class of modified gravity models, not necessary based on the Einstein-aether [34–36]. A detailed study of their impact on the CMB and matter power spectrum was performed in [10] with the following outcome:

(i) Whenever $G_{cos} \neq G_N$ the Poisson equation for sub-horizon scales in an expanding background is modified. As a result, the growth of sub-horizon perturbations is uniformly enhanced. For instance, during matter domination the density contrast behaves as (cf. [33])

$$\delta \propto a^{\frac{1}{4}(-1 + \sqrt{1 + 24G_N/G_{cos}})}.$$

This increases the amplitude and changes the slope of the LPS. As for the CMB, the main changes are a shift of the acoustic peaks due to an increase of the gravitational potential of the primordial plasma, and an enhancement of the integrated Sachs–Wolfe (ISW) effect at intermediate multipoles $10 \lesssim l \lesssim 100$. Note that the effects of enhanced gravity vanish to the leading order in the LV parameters in the Einstein-aether model once the condition (10b) of the absence of PN corrections is imposed. Indeed, in terms of the parameters α, β, λ the latter condition takes the form,

$$\alpha + \beta + 3\lambda = 0, \quad (25)$$

which is exactly the combination appearing in (24). On the other hand, in the khronometric case, enhanced gravity is compatible with the PN constraint (11).

(ii) The mode χ produces shear at superhorizon scales, which decays at later times. Interestingly, a non-zero coupling between the aether and DM postpones this decay [14]. The shear smoothes out the metric perturbations and leads to an overall suppression of the CMB anisotropies and LPS at the scales corresponding to the sound speed of the χ -mode, c_χ . This effect is partially degenerate with an overall rescaling of the amplitude of the primordial fluctuations and is only weakly constrained by the data.

Concerning the effects of type (iii), the main consequence of LV in DM is a scale-dependent modification of the growth rate of the density perturbations [14]. For modes with $k > k_{Y,0}/\sqrt{a(\tau)}$ the coupling to the aether violates the equivalence principle in the DM sector: the inertial mass of DM particles is smaller than their gravitational mass. This leads to an enhanced growth of the density contrast during matter domination,

$$\delta_{[dm]} \propto a^{\frac{1}{4}(-1 + \sqrt{25 + \frac{24\Omega_{dm}Y}{(\Omega_{dm} + \Omega_b)(1-Y)}})}. \quad (26)$$

On the other hand, the violation of the equivalence principle in DM is screened for modes with $k < k_{Y,0}/\sqrt{a(\tau)}$ and is almost absent at radiation domination. Thus, the total effect is a change of the slope of the LPS at $k > k_{Y,0}$. This is clearly visible in Fig. 1, upper panel, where we display the results of a numerical simulation of the LPS in the Λ LVDM model using the modified Boltzmann code CLASS [37]. The numerical values of the model parameters¹⁰ were chosen in a way to switch off the effects of enhanced gravity (i) and minimize the effects of the shear (ii),

$$\alpha = 0.005, \quad \beta = 0.025, \quad \lambda = -0.01, \quad Y = 0.5. \quad (27)$$

This corresponds to $k_{Y,0} = 1.14 \cdot 10^{-3} h \text{ Mpc}^{-1}$.

A comment on the definition of the power spectrum is in order. This definition is not obvious in the Λ LVDM model where both gravity and the dynamics of DM are modified leading to non-trivial relations between the density contrasts of DM, baryons and the fluctuations of the gravitational potential. In particular, the violation of the equivalence principle by DM at scales $k > k_{Y,0}/\sqrt{a}$ is accompanied by a bias factor [14],

$$\frac{\delta_{[b]}}{\delta_{[dm]}} = 1 - Y. \quad (28)$$

Therefore taking $\delta_{[dm]}$ or $\delta_{[b]}$ to compute the power spectrum would produce different results. Following [10] we use the Poisson equation to *define* the total density perturbation,

$$\delta\rho_{[tot]} = -\frac{k^2\phi}{4\pi G_N a^2}, \quad (29)$$

where ϕ is the perturbation of the Newtonian potential related to η and h by the standard formulas [31]. Then the power spectrum is defined as the ratio of this density perturbation to the *apparent* background density of DM and baryons. The latter differs from the true density entering the Friedmann equation due to the difference

¹⁰ For the standard cosmological parameters we take: $n_s = 1$, $h = 0.7$, $\Omega_b = 0.05$, $\Omega_{dm} = 0.25$, $A_s = 2.3 \cdot 10^{-9}$, and neglect the effects of reionization for illustrative purposes when computing the CMB spectrum.

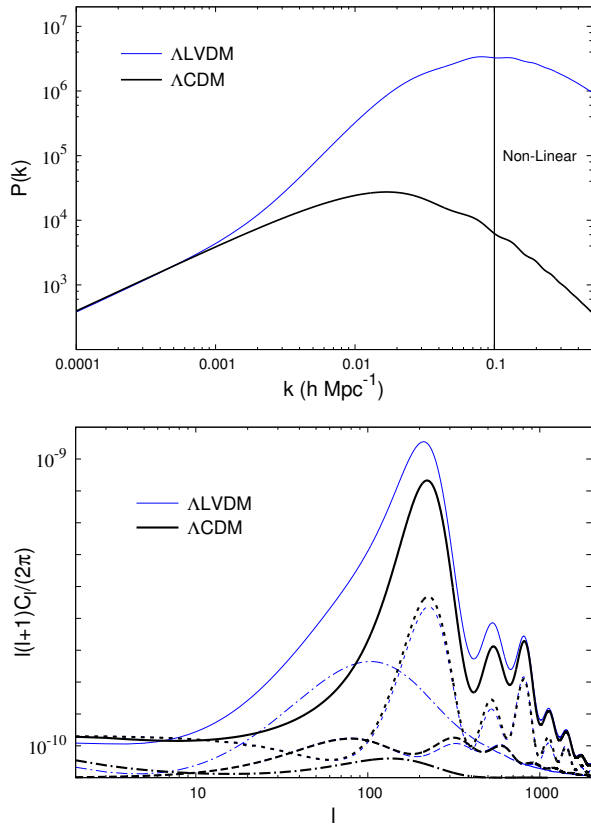


FIG. 1: *Upper panel:* Linear matter power spectrum in Λ CDM (thick black line) and ALVDM models (thin blue line) at redshift $z = 0$.

Lower panel: Temperature anisotropy spectrum (solid) and its decomposition in terms of Sachs–Wolfe (dotted), Doppler (dashed) and integrated Sachs–Wolfe (dot-dashed) contributions. Thick black lines represent the Λ CDM model, while thin blue lines are used for the ALVDM model.

between G_{cos} and G_N . Taking this into account, one obtains the final formula for the power spectrum [10],

$$P(k) = \left(\frac{G_N}{G_{cos}} \right)^2 \frac{\langle |\delta\rho_{[tot]}(\vec{k})|^2 \rangle}{\rho_{[dm]} + \rho_{[b]}}. \quad (30)$$

The definition (29) has a limited applicability: it is meaningful only well inside the Hubble horizon and for negligible shear. However, both conditions are satisfied for the range of wavenumbers where the power spectrum is actually measured. Taking the gravitational potential as the basis for the definition of LPS is motivated by the fact that this quantity is directly probed by the lensing surveys. The amount of galaxies and clusters is also believed to trace linearly the underlying gravitational field at large scales ($k < 0.1 h \text{ Mpc}^{-1}$), though contamination by a scale-dependent bias cannot be excluded (cf. [38]). A dedicated study of the clustering dynamics in the model at hand is required to definitely resolve this issue, which is beyond the scope of this paper.

A cleaner observable, insensitive to the above ambiguities, is the spectrum of CMB anisotropies. The temperature spectrum computed using CLASS in the model with the parameters (27) is shown in the lower panel of Fig. 1. The main modification comes from the very strong ISW effect induced by the accelerated growth of perturbations (26). It extends over a wide range of multipoles from $l \sim k_{Y,0}\tau_0$ (≈ 25 for the chosen parameters) up to $l \sim 1000$. Modifications in the Sachs–Wolfe and Doppler effects are small, consistent with the decoupling of DM from photon-baryon plasma at the epoch of recombination [39]. In particular, the positions of the acoustic peaks are not changed, which distinguishes the ALVDM impact on CMB from that of the modified Poisson equation (i) helping to break the degeneracy between them.

V. COMPARISON WITH DATA

The effects discussed above are constrained by the data on the CMB anisotropies and LPS. In this way the cosmological observations can be used to put bounds on LV in dark matter and gravity. For this purpose we use in this work the CMB data from the Planck 2013 release [12] combined with the galaxy power spectrum from the WiggleZ redshift survey [13]. To compute the predictions for observables at various values of the model parameters, we modify the Boltzmann code CLASS [37]. The parameter space is explored using the Monte Carlo code MONTE PYTHON [40]. We consider both Einstein-aether and khronometric models focusing only on the scalar sector of perturbations. We separately study the cases $Y \neq 0$ (Lorentz violation in dark matter) and $Y \equiv 0$ (dark matter is Lorentz invariant).

For non-zero Y the fit includes nine cosmological parameters, which are the usual six free parameters of the minimal flat Λ CDM model, plus three parameters describing LV in gravity and dark matter, namely $\log_{10} \alpha$, $\log_{10} c_\chi^2$ and Y . These combinations and the logscale have been chosen to improve the convergence of the Monte Carlo chains. For the last two parameters, we impose a flat prior in the ranges

$$0 \leq \log_{10} c_\chi^2, \quad 0 < Y < 1. \quad (31a)$$

The lower prior on $\log_{10} c_\chi^2$ follows from the Cherenkov bound discussed in Sec. III. We do not need an upper prior on $\log_{10} c_\chi^2$, as large values of c_χ^2 are strongly disfavored by the data, see Fig. 2. For given $\log_{10} \alpha$ and $\log_{10} c_\chi^2$, the parameters (β, λ) are fixed either by the condition (25) in the Einstein-aether case or by (11) for the khronometric model. We have seen that the effects of LV in DM are screened at wavenumbers smaller than $k_{Y,0} \propto \sqrt{Y/(\alpha c_\chi^2)}$. When $\alpha < 0.5 \cdot 10^{-5}$ (weak LV in gravity) one does not expect to obtain bounds on LV in DM from CMB or LPS: any $Y \sim 1$ is allowed because the screening occurs over the whole range of scales relevant for these observables (we take $k_{max} = 0.1 h \cdot \text{Mpc}^{-1}$ as

	$100 \omega_b$	ω_{cdm}	n_s	$10^{+9} A_s$	h	z_{reio}	α	c_χ^2	Y
E-ae	$2.225_{-0.031}^{+0.028}$	$0.1178_{-0.0022}^{+0.0025}$	$0.9635_{-0.0073}^{+0.0068}$	$2.159_{-0.050}^{+0.048}$	$0.683_{-0.012}^{+0.010}$	$10.4_{-1.0}^{+1.1}$	$< 5.0 \cdot 10^{-3}$	< 240	< 0.028
kh	$2.227_{-0.031}^{+0.028}$	$0.1174_{-0.0022}^{+0.0025}$	$0.9639_{-0.0072}^{+0.0068}$	$2.152_{-0.054}^{+0.048}$	$0.685_{-0.012}^{+0.010}$	$10.4_{-1.0}^{+1.1}$	$< 1.1 \cdot 10^{-3}$	< 55	< 0.029
E-ae, $Y \equiv 0$	$2.207_{-0.027}^{+0.026}$	$0.1200_{-0.0019}^{+0.0019}$	$0.9598_{-0.0063}^{+0.0062}$	$2.182_{-0.051}^{+0.045}$	$0.673_{-0.009}^{+0.009}$	$10.1_{-1.0}^{+1.0}$	$< 1.0 \cdot 10^{-2}$	< 427	—
kh, $Y \equiv 0$	$2.212_{-0.028}^{+0.027}$	$0.1191_{-0.0020}^{+0.0021}$	$0.9607_{-0.0066}^{+0.0067}$	$2.161_{-0.054}^{+0.053}$	$0.677_{-0.011}^{+0.009}$	$10.6_{-1.0}^{+1.1}$	$< 1.8 \cdot 10^{-3}$	< 91	—

TABLE I: Mean values and 68% CL minimum credible interval for the parameters of the ALVDM models. The first and third lines correspond to the Einstein-aether and the second and fourth lines — to the khronometric cases. For α , c_χ^2 and Y we give 95% CL upper limits. The bounds in the first two lines are subject to the priors (31).

the upper limit on the region where the power spectrum can be considered as linear). Thus, in order to obtain efficient constraints on Y , we impose a flat prior in the range¹¹

$$-4.7 < \log_{10} \alpha < 0.3 \quad (31b)$$

(which corresponds to $2 \cdot 10^{-5} < \alpha < 2$).

Our results for the marginalized Bayesian minimum credible intervals for the parameters of the fit are presented in the first two lines of Table I. The three LV parameters are found to be very weakly correlated with the usual Λ CDM parameters. The one-dimensional and two-dimensional posterior parameter distributions for LV parameters are displayed in Fig. 2. We see that the posterior distributions for $\log_{10} \alpha$, $\log_{10} c_\chi^2$ and Y are peaked at the lower ends of the scanned parameter space, implying that the data bring no evidence for LV. In particular, the parameter Y governing LV in the DM sector is constrained to be less than $Y < 0.03$ in both models. We stress, though, that this bound should be taken in conjunction with the priors (31). As we already explained, the linear observables become insensitive to LV in DM for very small values of α . The data on non-linear structure can presumably help to find constraints in this regime. However, this requires an analysis of the non-linear dynamics of the model, which is beyond the scope of the present paper.

We observe a triangular shape for the allowed region in the $(\log_{10} \alpha, \log_{10} c_\chi^2)$ plane. One concludes that the data essentially constrain the combination αc_χ^2 entering $k_{Y,0}$ by disfavoring models where the enhanced growth of structure due to LV in DM takes place on linear scales. This implies that the introduction of a non-zero parameter Y in the fit biases the combination αc_χ^2 towards

smaller values. Therefore, the bounds on α and c_χ^2 from the first two lines in Table I do not apply to the case when LV is confined to the gravitational sector only and DM is exactly Lorentz invariant ($Y \equiv 0$ from the start). To obtain the constraints in this case we ran separate series of simulations setting $Y = 0$ in all dynamical equations. Otherwise we followed the same procedure as before. We varied $\log_{10} \alpha$ and $\log_{10} c_\chi^2$ in addition to the six standard Λ CDM parameters, with the priors (31). The resulting posterior distributions for the parameters $(\log_{10} \alpha, \log_{10} c_\chi^2)$ are shown in Fig. 3 and the marginalized credible intervals are listed in the last two lines of Table I. One observes that the new bounds are indeed weaker than in the case of LV DM.

For the khronometric model (Fig. 3, lower panel) the isoprobability contours have the same shape as in the case of ALVDM implying that the constrained combination is again αc_χ^2 . This is consistent with the expectation that the main effects in this case are related to the difference between G_N and G_{cos} (type (i) according to the classification of Sec. IV). Imposing the PN constraint (11) one obtains,

$$\frac{G_N}{G_{cos}} - 1 = \frac{3}{2} \alpha c_\chi^2, \quad (32)$$

where we have used (24) and the first formula in (20). This is the combination mostly constrained by the data. Note that the bound on α obtained in this paper is 50 times better than a bound derived in Ref. [10] for a similar model (the bound in [10] is formulated in terms of $\beta = \alpha/2$ and reads $\beta < 0.05$). This is a consequence of the reduction of the parameter space after imposing the Cherenkov radiation constraint $c_\chi \geq 1$. Another source of improvement is the use of more recent CMB data (Planck 2013 vs. WMAP 7 and SPT in [10]).

In the Einstein-aether case (Fig. 3, upper panel) the bounds on α and c_χ^2 are significantly weaker. This is explained by the observation made in Sec. IV that, once the relevant PN constraint (25) is imposed, the effects of enhanced gravity disappear and we are left with the effects of the type (ii) related to the shear sourced by the aether. These effects are proportional to $\beta = \alpha(1 + 3c_\chi^2)/2$ and are rather suppressed, which translates into mild bounds on α and c_χ^2 . Note, however, that the bound on α is still at the per cent level, which is comparable with

¹¹ We have found that the linear observables remain sensitive to the effects of LV in DM even for $k_{Y,0}$ somewhat above k_{max} , suggesting that some constraints on Y could be obtained down to the values $\alpha \sim 10^{-7}$. However, for large $k_{Y,0}$ the last term in brackets in eq. (19) leads to fast oscillations of the χ -field and the numerical computations become very demanding. Our decision to impose the stronger priors (31b) represents a compromise between the desire to explore the physically interesting portion of the parameter space and computational efficiency.

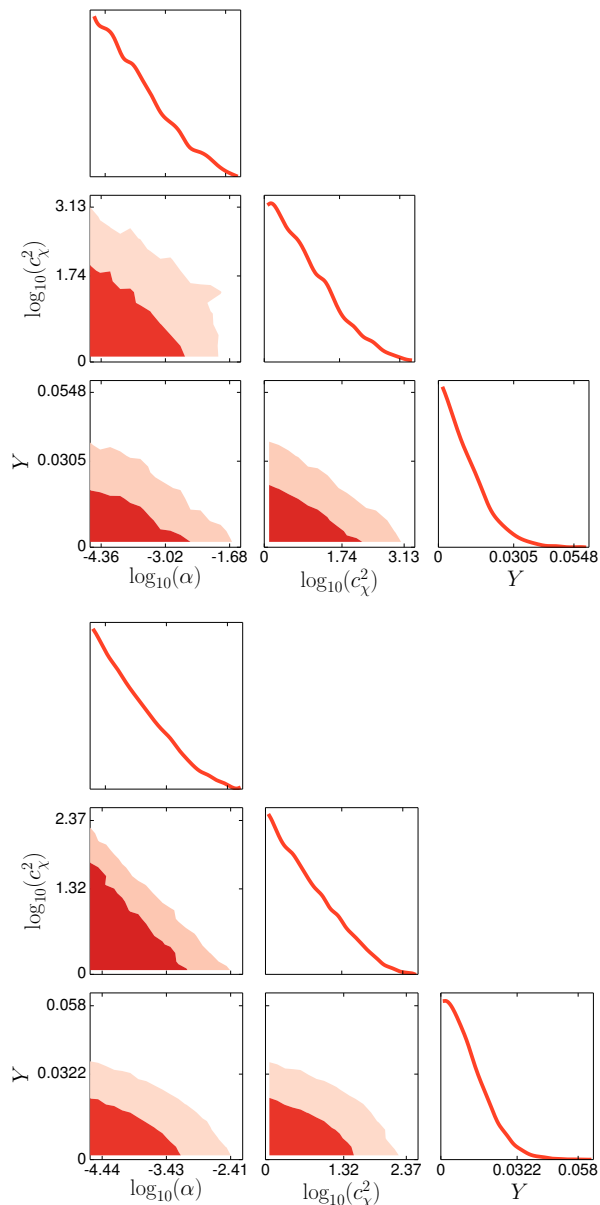


FIG. 2: Marginalized one-dimensional posterior distribution and two-dimensional probability contours (at the 68% and 95% CL) of the ALVDM parameters for Einstein-aether (upper panel) and khronometric (lower panel) cases. Only the subspace of parameters responsible for Lorentz violation is shown.

the bounds from binary pulsars [4].

VI. CONCLUSIONS

In this paper we have used the Planck 2013 and WiggleZ 2012 data to derive constraints on the deviations from Lorentz invariance in gravity and dark matter. We considered the scenario where local Lorentz invariance

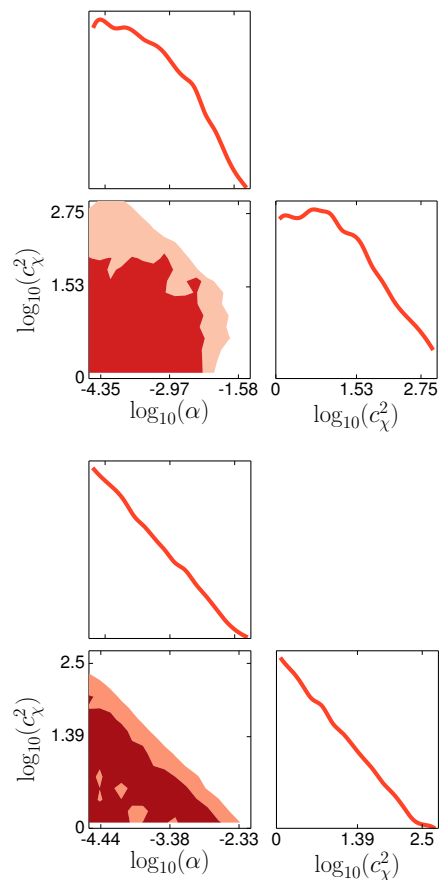


FIG. 3: Marginalized one-dimensional posterior distribution and two-dimensional probability contours (at the 68% and 95% CL) of the parameters for Einstein-aether (upper panel) and khronometric (lower panel) theories in the case of Lorentz invariant dark matter ($Y \equiv 0$). Only the subspace of parameters responsible for Lorentz violation is shown.

is broken down to spatial rotations preserving a time-like direction. This pattern of symmetry breaking is described at low energies by the Einstein-aether or khronometric model. The latter case represents the infrared limit of Hořava gravity. We allowed for a possible LV coupling between aether (khronon) and dark matter keeping Lorentz invariance in the sectors of the Standard Model and dark energy (accounted for by a cosmological constant).

While for the background cosmological evolution the resulting ALVDM model is almost equivalent to Λ CDM, the difference is substantial at the level of perturbations. We studied the impact of these differences on the CMB and LPS using the modified Boltzmann code CLASS [37], and explored the parameter space of ALVDM with the parameter inference code MONTE PYTHON [40]. We performed four series of Monte Carlo simulations for the Einstein-aether and khronometric cases with and without LV in dark matter. In the analysis we imposed as

priors the constraints from local gravitational measurements in the Solar System and the astrophysical bound following from the absence of vacuum Cherenkov losses by ultra-high energy cosmic rays. As a result we have obtained the most stringent constraints to date on the departures from Lorentz invariance in cosmology. Our limits on the parameters of LV in the gravity sector are competitive with those coming from the slow-down of binary pulsars [4]. The dimensionless parameter Y characterizing LV in dark matter has been constrained to be less than 0.03. This parameter has the meaning of the difference between the maximal velocity¹² of dark matter particles and the speed of light. Our analysis provides the first direct constraint on this quantity.

It should be emphasized, however, that the latter constraint applies only under the priors (31) imposed to keep the effects of LV in dark matter unscreened in the linear regime. When the screening happens, CMB and LPS get insensitive to the parameter Y . It will be interesting¹² Here, we are referring to the maximal velocity that DM particles could reach in principle in the ultra-relativistic limit, and not to

ing to investigate if in this regime LV dark matter can still be tested through the properties of the non-linear structures, such as e.g. the halo mass function.

In our analysis we focused on the scalar sector of perturbations. The presence of vector excitations in the Einstein-aether case can affect the CMB polarization, including the B-mode [29, 30]. We leave the study of the corresponding constraints for the future.

Acknowledgments. We are grateful to Grigory Rubtsov and Oleg Ruchayskiy for useful discussions. The numerical simulations were partially performed at the cluster of the Theoretical Division of INR RAS. This work was supported in part by the Swiss National Science Foundation (B.A., M.I., J.L., S.S.). M.I. also acknowledges support from the Grants of the President of Russian Federation MK-1754.2013.2, NS-2835.2014.2, and the RFBR grants 14-02-31435 and 14-02-00894.

actual DM velocities in the Universe during matter domination.

-
- [1] V. A. Kostelecky and N. Russell, *Rev. Mod. Phys.* **83** (2011) 11 [arXiv:0801.0287 [hep-ph]].
- [2] S. Liberati, *Class. Quant. Grav.* **30**, 133001 (2013) [arXiv:1304.5795 [gr-qc]].
- [3] C. M. Will, *Living Rev. Rel.* **17**, 4 (2014) [arXiv:1403.7377 [gr-qc]].
- [4] K. Yagi, D. Blas, N. Yunes and E. Barausse, *Phys. Rev. Lett.* **112**, 161101 (2014) [arXiv:1307.6219 [gr-qc]]; *Phys. Rev. D* **89**, 084067 (2014) [arXiv:1311.7144 [gr-qc]].
- [5] P. Horava, *Phys. Rev. D* **79**, 084008 (2009) [arXiv:0901.3775 [hep-th]].
- [6] D. Blas, O. Pujolas and S. Sibiryakov, *Phys. Rev. Lett.* **104** (2010) 181302 [arXiv:0909.3525 [hep-th]].
- [7] T. Jacobson and D. Mattingly, *Phys. Rev. D* **64**, 024028 (2001) [arXiv:gr-qc/0007031].
- [8] D. Colladay and V. A. Kostelecky, *Phys. Rev. D* **58** (1998) 116002 [hep-ph/9809521].
- [9] J. A. Zuntz, P. G. Ferreira and T. G. Zlosnik, *Phys. Rev. Lett.* **101**, 261102 (2008) [arXiv:0808.1824 [gr-qc]].
- [10] B. Audren, D. Blas, J. Lesgourgues and S. Sibiryakov, *JCAP* **1308** (2013) 039 [arXiv:1305.0009 [astro-ph.CO]].
- [11] D. Blas and S. Sibiryakov, *JCAP* **1107** (2011) 026 [arXiv:1104.3579 [hep-th]].
- [12] P. A. R. Ade *et al.* [Planck Collaboration], arXiv:1303.5062 [astro-ph.CO].
- [13] D. Parkinson, S. Riemer-Sorensen, C. Blake, G. B. Poole, T. M. Davis, S. Brough, M. Colless and C. Contreras *et al.*, *Phys. Rev. D* **86**, 103518 (2012) [arXiv:1210.2130 [astro-ph.CO]].
- [14] D. Blas, M. M. Ivanov and S. Sibiryakov, *JCAP* **1210**, 057 (2012) [arXiv:1209.0464 [astro-ph.CO]].
- [15] T. Jacobson, *PoS QG-PH*, 020 (2007) [arXiv:0801.1547 [gr-qc]].
- [16] D. Blas, O. Pujolas, S. Sibiryakov, *JHEP* **1104**, 018 (2011) [arXiv:1007.3503 [hep-th]].
- [17] T. Jacobson, “Undoing the twist: the Hořava limit of Einstein-aether,” arXiv:1310.5115 [gr-qc].
- [18] S. Groot Nibbelink and M. Pospelov, *Phys. Rev. Lett.* **94**, 081601 (2005) [hep-ph/0404271].
- [19] O. Pujolas and S. Sibiryakov, *JHEP* **1201**, 062 (2012) [arXiv:1109.4495 [hep-th]].
- [20] G. Bednik, O. Pujolas and S. Sibiryakov, *JHEP* **1311**, 064 (2013) [arXiv:1305.0011 [hep-th]].
- [21] S. R. Coleman and S. L. Glashow, *Phys. Rev. D* **59**, 116008 (1999) [hep-ph/9812418].
- [22] N. Andersson and G. L. Comer, *Living Rev. Rel.* **10** (2007) 1 [gr-qc/0605010].
- [23] S. Dubovsky, T. Gregoire, A. Nicolis and R. Rattazzi, *JHEP* **0603**, 025 (2006) [hep-th/0512260].
- [24] D. Blas and H. Sanctuary, *Phys. Rev. D* **84** (2011) 064004 [arXiv:1105.5149 [gr-qc]].
- [25] L. Shao, R. N. Caballero, M. Kramer, N. Wex, D. J. Champion and A. Jessner, *Class. Quant. Grav.* **30** (2013) 165019 [arXiv:1307.2552 [gr-qc]].
- [26] J. Bovy and G. R. Farrar, *Phys. Rev. Lett.* **102**, 101301 (2009) [arXiv:0807.3060 [hep-ph]].
- [27] S. M. Carroll, S. Mantry, M. J. Ramsey-Musolf and C. W. Stubbs, *Phys. Rev. Lett.* **103**, 011301 (2009) [arXiv:0807.4363 [hep-ph]]; S. M. Carroll, S. Mantry and M. J. Ramsey-Musolf, *Phys. Rev. D* **81**, 063507 (2010) [arXiv:0902.4461 [hep-ph]].
- [28] S. M. Carroll and E. A. Lim, *Phys. Rev. D* **70**, 123525 (2004) [arXiv:hep-th/0407149].
- [29] C. Armendariz-Picon, N. F. Sierra and J. Garriga, *JCAP* **1007** (2010) 010 [arXiv:1003.1283 [astro-ph.CO]].
- [30] M. Nakashima and T. Kobayashi, *Phys. Rev. D* **84**, 084051 (2011) [arXiv:1103.2197 [astro-ph.CO]].
- [31] C. P. Ma and E. Bertschinger, *Astrophys. J.* **455** (1995) 7 [arXiv:astro-ph/9506072].
- [32] J. W. Elliott, G. D. Moore and H. Stoica, *JHEP* **0508**, 066 (2005) [hep-ph/0505211].
- [33] T. Kobayashi, Y. Urakawa and M. Yamaguchi, *JCAP* **1004**, 025 (2010) [arXiv:1002.3101 [hep-th]].
- [34] T. Clifton, P. G. Ferreira, A. Padilla and C. Sko-

- rdis, Phys. Rept. **513**, 1 (2012) [arXiv:1106.2476 [astro-ph.CO]].
- [35] L. Amendola *et al.* [Euclid Theory Working Group Collaboration], Living Rev. Rel. **16**, 6 (2013) [arXiv:1206.1225 [astro-ph.CO]].
- [36] I. D. Saltas, I. Sawicki, L. Amendola and M. Kunz, “Scalar anisotropic stress as signature of correction to gravitational waves,” arXiv:1406.7139 [astro-ph.CO].
- [37] D. Blas, J. Lesgourgues and T. Tram, JCAP **1107** (2011) 034 [arXiv:1104.2933 [astro-ph.CO]].
- [38] F. Villaescusa-Navarro, F. Marulli, M. Viel, E. Branchini, E. Castorina, E. Sefusatti and S. Saito, JCAP **1403**, 011 (2014) [arXiv:1311.0866 [astro-ph.CO]].
- [39] L. Voruz, J. Lesgourgues and T. Tram, JCAP **1403**, 004 (2014) [arXiv:1312.5301 [astro-ph.CO]].
- [40] B. Audren, J. Lesgourgues, K. Benabed and S. Prunet, JCAP **1302**, 001 (2013) [arXiv:1210.7183 [astro-ph.CO]].
- [41] M. M. Ivanov and S. Sibiryakov, JCAP **1405**, 045 (2014) [arXiv:1402.4964 [astro-ph.CO]].